Geomechanics and Engineering, *Vol. 39, No. 3 (2024) 211-226*
https://doi.org/10.12989/gae.2024.39.3.211

Experimental study on the mechanical behaviors of rigid pile composite foundation in Yellow River alluvial plain upon ground water level fluctuations

Yunlong Liu, Chongxuan Yuan, Lei Wang* and Sihua Zhang

Zhengzhou University, Zhengzhou, Henan, 450066, China

(*Received June 24, 2021, Revised August 23, 2024, Accepted September 16, 2024*)

Abstract. In recent years, the increasingly frequent extreme weather conditions in Yellow River Alluvial Plain (YRAP) like heavy rains and drought have resulted in significant Ground Water Level (GWL) fluctuations. After long-distance transportation by Yellow River, the silt in this area gains characteristics of high particle roundness and poor grain gradation, which makes it sensitive to the changes of water content. Consequently, upon GWL fluctuations, the bearing behaviors of Rigid Pile Composite Foundation (RPCF) gradually deteriorate and result in additional settlement. In order to investigate the changing disciplines and inherent mechanisms of the RPCF bearing behaviors upon GWL fluctuations, a large-scale model test was performed and presented. The experimental results suggest that RPCF settlement experiences a sudden increase in the first GWL fluctuation cycle and then gradually stabilizes in the following cycles. Such phenomenon could be attributed to the soil structure rearrangement induced by matric suction reduction in the GWL rise process and growth of effective stress in the GWL drop process. Further, considering the soil stiffness deterioration in the GWL rise process, the traditional composite modulus method for RPCF settlement estimation was modified to extend its application in unsaturated YRAP. The changing disciplines, mechanisms and estimation method presented can facilitate practicing engineers to gain a more comprehensive understanding on the bearing behaviors of RPCF in YRAP upon GWL fluctuations.

Keywords: bearing capacity; ground water level fluctuation; matric suction; rigid pile composite foundation; Yellow River alluvial plain

1. Introduction

The Yellow River basin in China is characterized by concentrated rainfall and serious floods. Years later, it makes southwest provinces flooding deposition areas. This region covers an area up to around 250,000 km^2 and is commonly known as Yellow River Alluvial Plain (YRAP) (Cheng 2001, Song 2010, Jin 2020). There are numerous national central and prefecture-level cities located in YRAP.

At the same time, several key high-speed railway lines and national strategic projects including West-East Gas Transmission Project Line and West to East Power Transmission Project Line also pass through this region, as shown in Fig. 1(a). In YRAP, the silt brought by the Yellow River from the upper reaches deposits in the lower reaches, as shown in Figs. 1(b) and 1(c). Due to the long-distance transportation of Yellow River, the silt in this region gains the characteristics of high silt content, high particle roundness and poor gradation (Song 2010, Yao 2006, Xiao 2008, Jin 2020), which make its engineering properties extremely sensitive to water content variations. In recent years, the increasingly frequent extreme weathers like heavy rains and drought has resulted in considerable GWL fluctuation in YRAP. Consequently, both the strength and stiffness of the silt gradually degrades in this process, so as to causes a series of engineering problems such as subsidence of railway subgrade, differential settlement of building foundation and slide of foundation pit, as shown in Fig. 1(d).

Fig. 2 illustrates the evolution of the microstructure of the silt in YRAP during the rise and drop of GWL. Due to the poor particle gradation and high particle roundness, large pores are formed between soil particles and filled with air and water in an unsaturated state, as shown in Fig. 2(a). The water in the pore adheres to the soil particle surface or sticks to the contact point of soil particles. The surface tension generated by the capillary water at the contact point prevents the sliding between soil particles, thus improving the stiffness and strength of soil. Hence the settlement of foundations constructed on it can be controlled within an allowable range under service load, as shown in Fig. 2(b). However, once the GWL rises and water content increases, the lubrication effect of water increases and the capillary effect of water disappears. The soil structure can no longer be maintained due to the vanishment of surface tension. The soil may suffer collapsed settlement under upper load due to the strength and stiffness degradation, as shown in Fig. 2(c) (Cheng 2001, Fan 2007, Song 2010). Furthermore, if the GWL drops, the pore water will flow out, taking away the fine particles in the pores. The soil particles will be rearranged under the increasing effective stress, a minor consolidation settlement can be observed as shown in Fig. 2(d). The surface tension will be generated again to support the newly formed soil skeleton structure.

*Corresponding author, Ph.D.
E-mail: lwang029@zzu.edu.cn

ISSN: 2005-307X (Print), 2092-6219 (Online)

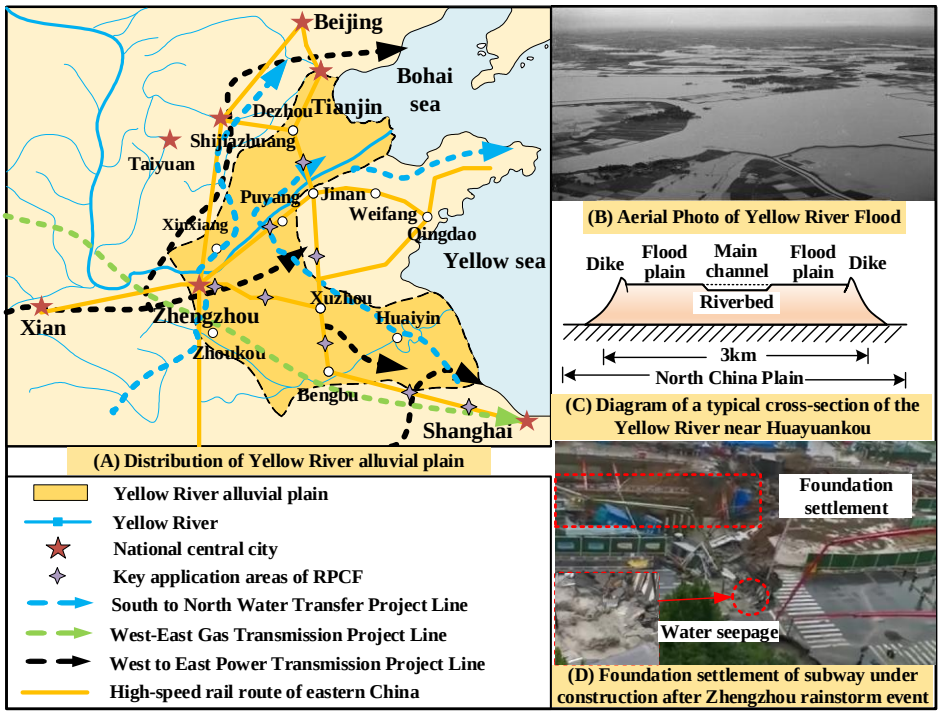

Fig. 1 Distribution of YRAP and various engineering problems in this area

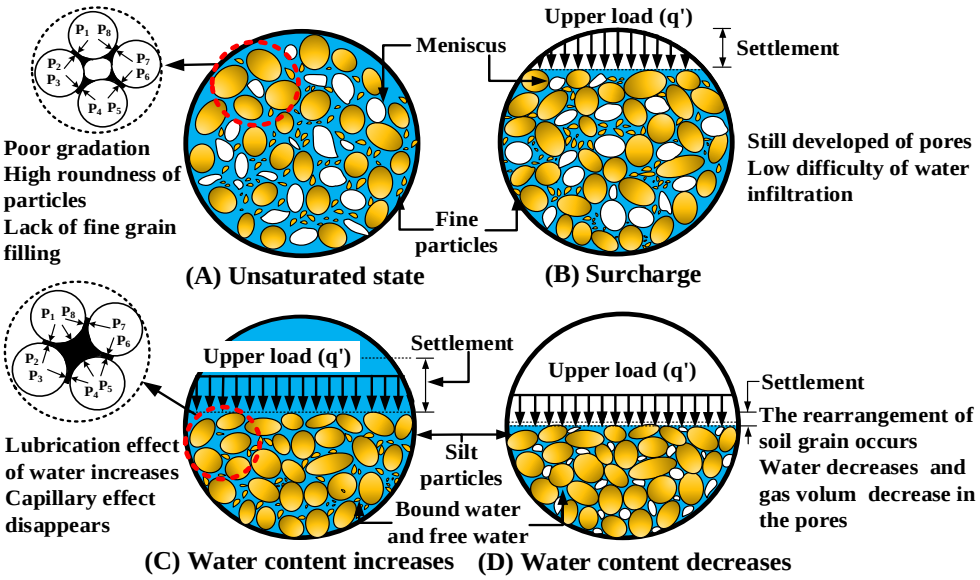

Fig. 2 Diagram of microstructure evolution of the silt in YRAP

According to the formation process, the YRAP silt can be classified as silt in plain area and aqueous silty silt. Table 1 summarizes the shear strength parameters of different types of silt. Due to the poor gradation (low clay content) and high roundness, the internal friction angle and cohesion of the YRAP silt are generally smaller than those of weathered silty silt, residual silty silt and mountain silty silt.

The rigid pile composite foundation (RPCF) gains good economic and social benefits by making full use of the bearing capacity of soil between piles (e.g., Bie 2014, Sharma 2015, Zhang 2018, Chen 2019, Fu *et al*. 2020).

Therefore, this type of foundation has been widely used in YRAP. Currently, the design and research on RPCF in YRAP is commonly based on the saturated soil mechanics. However, the soil between piles is typically in a condition of unsaturated state. The soil water content can change periodically with the GWL fluctuations induced by either natural weather changes like rainstorm and drought (An *et al.* 2013, Yu 2022) or artificial activities like excessive groundwater exploitation and agricultural irrigation. In this process, the RPCF bearing behaviors gradually deteriorate due to soil mechanical properties degradation, so as to give

Table 1 Shear strength of various silts in saturated state or nearly-saturated state

Name		Typical species	Internal friction angle/°	Cohesion/kPa
Weathered silty silt		Collapsible loess (Pan 2018)	20.84	22.70
Residual silty silt		Basalt residual soil (Li *et al.* 2018)	15.3	25
Aqueous silty silt	Mountain silty silt	Silty sand from the Swiss Molasse (Schnellmann *et al.* 2013)	33.7	23
	Silt in plain area	YRAP silt (Li *et al.* 2022)	13.38	16.12

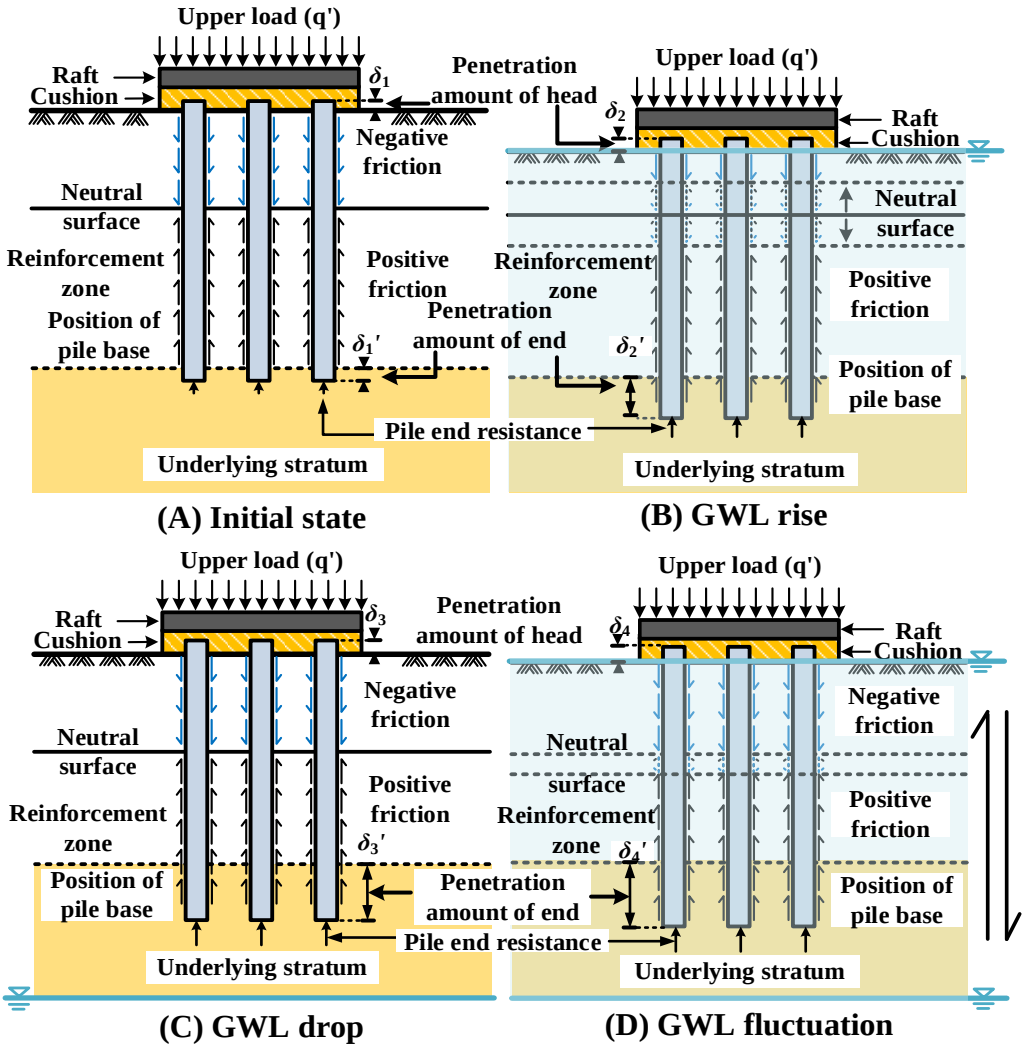

Fig. 3 Influence of GWL fluctuations on RPCF in YRAP

rise to a series of engineering problems.

As shown in Fig. 3(a), prior to GWL fluctuations, the upper load is shared by the piles and soil between piles. The neutral surface indicating the same pile and soil settlement and zero pile shaft friction is located at the upper part of the pile. Negative friction generates above the neutral surface while positive friction generates below it. Once the GWL rises, as shown in Fig. 3(b), more load is born by the pile due to soil mechanical properties degradation. The compression deformation of both the soil in the reinforcement zone and underlying soil stratum increase significantly. As a consequence, the RPCF suffers additional settlement. The position of the neutral surface may move upward or downward depending on the pile-soil relative displacement relationship. When the GWL drops, the flow away of fine soil particles together with water seepage and the rearrangement of large soil particles under the influences of increasing effective stress contribute to the additional RPCF consolidation settlement. The neutral surface further moves down, as shown in Fig. 3(c). Along with cyclic GWL fluctuations, both the pile and soil mechanical behaviors changes periodically with periodic changes of pore water pressure. Eventually a irreversible process forms and no additional settlement can be observed with GWL fluctuations cycle increment, as shown in Fig. 3(d).

Table2 Typical experiment of RPCF

References	Boundary conditions (stress and displacement)	Typical experimental device diagram	Influencing factors	Conclusions
Yang and Wang (2010)	The upper load is 180 kPa	Fig. 4(a)	Pile spacing	Pile spacing is an important factor influencing bearing behavior. A proper pile spacing and arrangement should be considered in the design.
Sun (2010)	Load differential in static load test is 65 kPa	Fig. 4(b)	Foundation stiffness	With the increase of foundation stiffness, the bearing capacity efficiency factors of pile increases gradually
Liu *et al*. (2015)	The maximum value of pile head load is 418.6 kPa, the thickness of the cushion layer is 100~ 500 mm and the deformation modulus is 40~140 MPa	Fig. 4(c)	Thickness of cushion	Settlement increases with the increase of cushion thickness, while pile-soil stress ratio decreases
			Deformation modulus of cushion	Settlement decreases with the increase of deformation modulus of cushion, and the pile-soil stress ratio increases with the increase of deformation modulus of cushion.
Liu *et al*. (2016)	The pile head load is from 12 to 124 kPa, and the dimensions of bearing plate are 0.15 m, 0.25 m, 0.4 m and 0.5 m	Fig. 4(d)	The size of bearing plate	When the area replacement ratio of soil around piles to piles and the contact stress of soil under the pile is the same, the RPCF settlement increases with the increase of the size of bearing plate
Xu (2020)	Applied side load are 50kPa, 100kPa and 150kPa	Fig. 4(e)	The side load	The higher the side load, the greater the bearing capacity of the composite foundation, but when the characteristic value of the bearing capacity of the composite foundation is reached, the bearing capacity of the composite foundation pile is gradually reduced.
Cai (2021)	The designed maximum load of the two tests were both set to be 2,800N	Fig. 4(f)	Pile material	Compared with the impervious pile, the pervious pile can significantly accelerate the dissipation of excess pore water pressure after pile installation

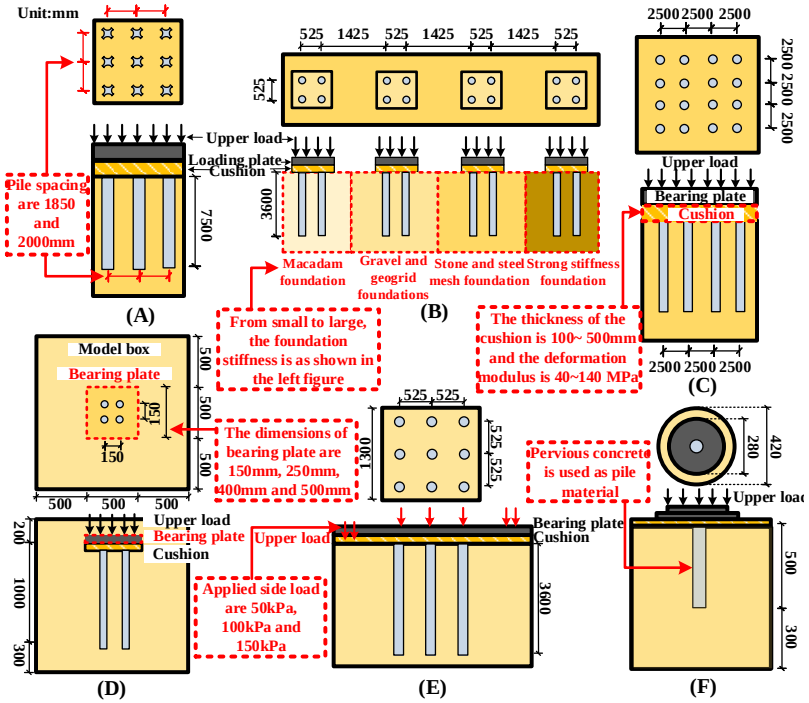

Fig. 4 Representative experimental settings of RPCF under different stress and displacement boundary conditions

Although the increasing numbers of engineering problems of RPCF have been reported, few attentions have been focused on the changing patterns and mechanisms of bearing behaviors of RPCF upon GWL fluctuations (Zhang *et al.* 2017). In this study, a large-scale model test on RPCF under service load subjected to GWL fluctuations was designed and performed. The variation law of the pile-soil stress ratio, soil pressure beneath the cushion, pile head load, pile shaft friction and pile base resistance were revealed and the changing mechanisms were analyzed using the saturated and unsaturated soil mechanics. A revised composite modulus method was further proposed for the prediction of RPCF settlement, which can serve the design and long-time performance evaluation of RPCF in YRAP.

GWL fluctuations generally exists in engineering practice. Many scholars have paid close attention to the detrimental effects of GWL fluctuation on existing buildings (Hansen *et al*.1987, Reddy and Manjunatha 1997, Ausilio *et al*. 2005, Luo *et al.* 2011, Veiskarami and Kumar 2012, Kumar and Chakraborty 2013, Zhao *et al*. 2014,

Ajdari and Esmail 2015, Dong *et al*. 2016, Park *et al.* 2019, Lu *et al.* 2020, Alencar *et al*. 2021). For example, with the change of GWL, the bearing behaviors of shallow foundation, deep foundation and RPCF decreases significantly (Dong *et al.* 2016, Park *et al.* 2017). Recently, some scholars discussed the influencing mechanism of GWL fluctuation on these foundations. As the GWL rises, the foundation settlement may increase by several times rapidly and such settlement is mainly plastic and irreversible. The key factor responsible for additional settlement is the degradation of soil mechanical properties due to water content increment (Wang *et al*. 2015, Park *et al.* 2019). As the GWL drops, the foundation settlement can gain a relatively small consolidation increment due to the increase of effective stress (Safarzadeh *et al*. 2019, Fu 2019). After several cycles of GWL fluctuations, the settlement of foundations shows minor changes with pore water pressure changes (Zhang *et al.* 2021). However, till now few researches are available discussing the bearing behavior changes of foundations in YRAP upon GWL fluctuations.

3. Materials and methods

3.1 Model test of RPCF upon GWL fluctuations

3.1.1 Index and mechanical properties of the silt in YRAP

The silt used in the model test was collected from Zhengzhou city located in YRAP, where the RPCF has been widely used. Following ASTM standards, the soil index properties were obtained and presented Table 3.

The soil water characteristic curve (SWCC) of the YRAP silt was measured using pressure plate method following ASTM-D6836-16. The Fredlund and Xing (1994) model was used to fit the SWCC, which is shown in Eq. (1). The experimental data, fitting curve and fitting parameters are shown in Fig. 5.

$$S_r = 100 \times \frac{\left[1-\ln\left(1+s/s_{re}\right)/\ln\left(1+10^6/s_{re}\right)\right]}{\ln\left[e+\left(s+a\right)^m\right]^n} \quad (1)$$

where S_r is soil saturation degree; s is the matric suction measured in the experiment; s_{re} is the measured residual suction; a, m, n are fitting parameters

The pile-soil interface shear strength were obtained through interface direct shear test. More specifically, initially an aluminum block was fabricated which met the size requirement of the direct shear apparatus. Then, sand paper was pasted on the aluminum block to create a rough surface like the model pile. Thirdly, a series of interface direct shear tests were performed under different normal stresses (i.e., 25, 50, 100 and 200 kPa) and volumetric water content (i.e., 12.8%, 22.4%, 32% and 40%). According to the SWCC shown in Fig. 5, the corresponding matric suctions of these water content are 327, 141, 45 and 0 kPa, respectively. The dry density of the soil is set as 1600 kg/m^3 according to the site investigation results. Based on a specific gravity of 2.705, the void ratios after compaction under four different levels of water content mentioned above were calculated to be 0.78, 0.73, 0.69 and 0.67, respectively. Consolidated drained test was performed for the saturated interface shear test and the shear rate was set as 0.02mm/min. Following the measurements, it was determined that the alterations in both the void ratio and volumetric water content of the soil after consolidation were insignificant and can be disregarded. For the unsaturated interface shear test, all the gaps of the shear chamber were covered with wet cottons to avoid any possible moisture loss in the testing process. Also, quick shear (1mm/min) was performed to enable the sample to be sheared to failure under a constant water content

The relationship between shear stress and shear displacement of four different water contents are shown in Fig. 6. It can be seen that the shear stress of the interface shear test increases nonlinearly with the shear displacement. In addition, the peak shear stress during the test is taken as the interface shear strength of silt concrete, and the corresponding shear displacement at failure increases with the increase of normal stress. Fig. 7 indicates the development of the peak interface shear strength with net normal stress and matric suction.

According to Hamid and Miller (2009), the interface shear strength parameters can be estimated using Eq. (2). In this equation, the first two terms indicate the contribution of true cohesion and net normal stress to the pile shaft friction while the last term indicates the contribution of matric suction to

Table 3 Index properties of silt in YRAP

Properties	Value	References
Natural water content /%	10	Specific gravity test (ASTM D854-14)
Specific gravity G_s	2.705	
Liquid limit, *LL* (%)	27.2	Atterberg limits test (ASTM D4318-10-e1)
Plastic limit, *PL* (%)	19.1	
Plastic index, *PI*	8.1	
Maximum dry unit weight, $\gamma_{d,max}$ (kg/m^3)	1850	Compaction curve (ASTM,12 400ft-lbf/ft3 (600 kN-m/m3) (ASTM D698-12e2)
Optimum water content, *w* (%)	13	
Elastic modulus under saturated condition, E_{sat} (MPa)	0.145	One-dimensional oedometer compression test (ASTM D3999/D3999M-11e1)
Elastic modulus under unsaturated condition of 13.5% water content, E_{unsat} (MPa)	2.48	

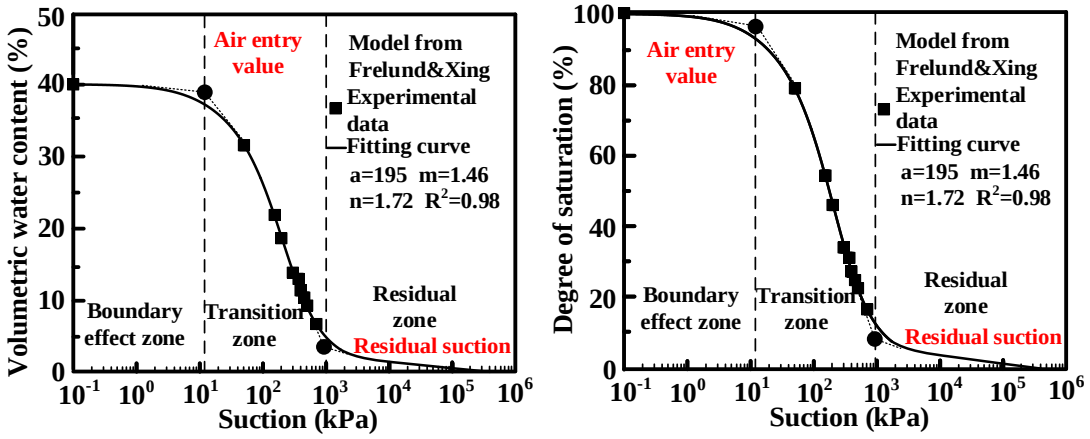

Fig. 5 SWCC of the YRAP silt and fitting curve

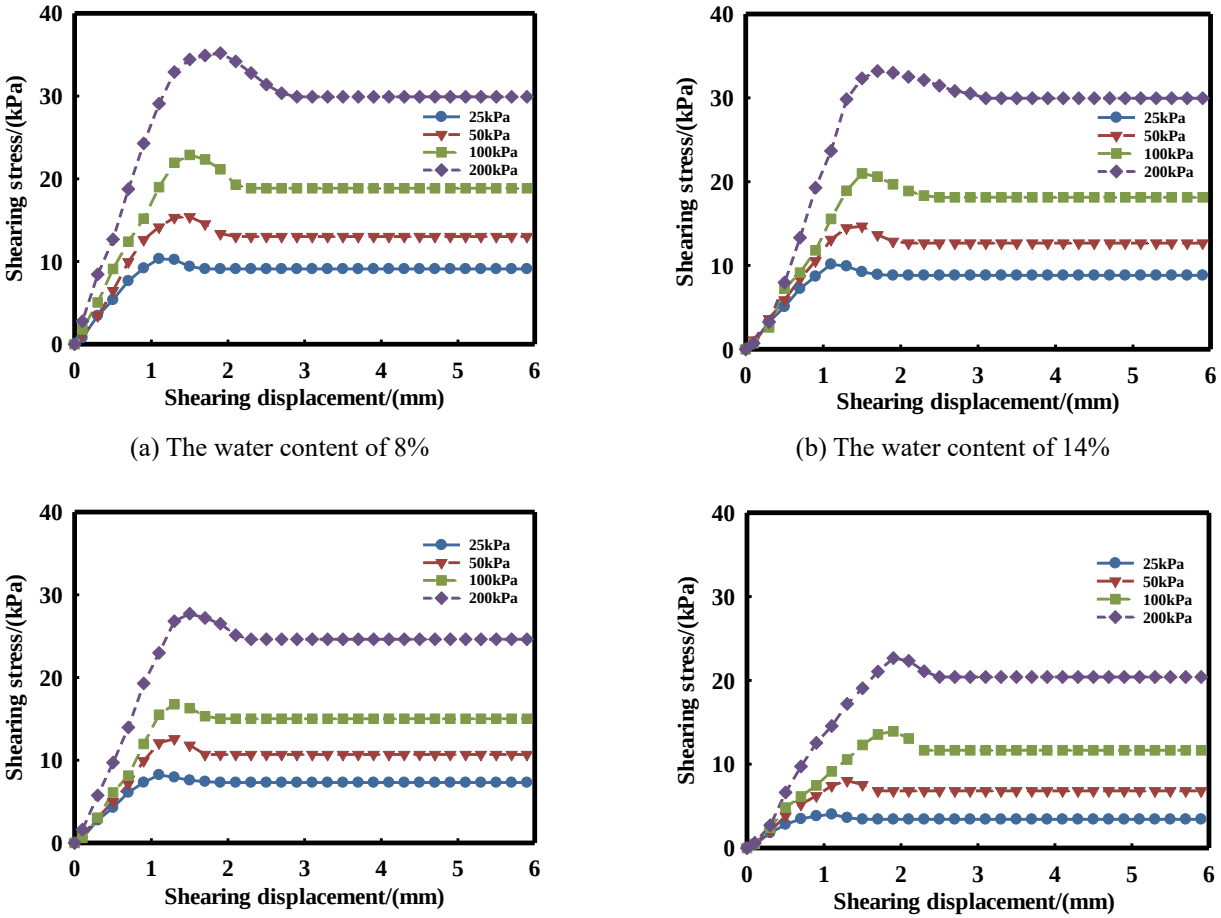

(a) The water content of 8%

(b) The water content of 14%

(c) The water content of 20%

(d) The saturated water content

Fig. 6 Shear-displacement curves of silt interface under different water content conditions

the pile shaft friction. Using Eq. (2), the interface shear strength parameters $\delta^{'}$, δ^{b}, $c_a^{'}$ were calculated as 10.93°, 6.41°and 3.45 kPa respectively

$$\tau_{su} = c_a^{'} + (\sigma_{nf} - u_{af})\tan\delta^{'} + (u_{af} - u_{wf})\tan\delta^{b} \quad (2)$$

where $c_a^{'}$ is the effective adhesion intercept for the interface; $\delta^{'}$ is the interface friction angle with respect to net normal stress; δ^{b} is the interface friction angle with respect to matric suction; (σ_{nf}-u_{af}) is the net normal stress at failure; (u_{af}-u_{wf}) is the matric suction at failure.

3.1.2 Experimental settings

The scheme of the newly designed testing box is shown in

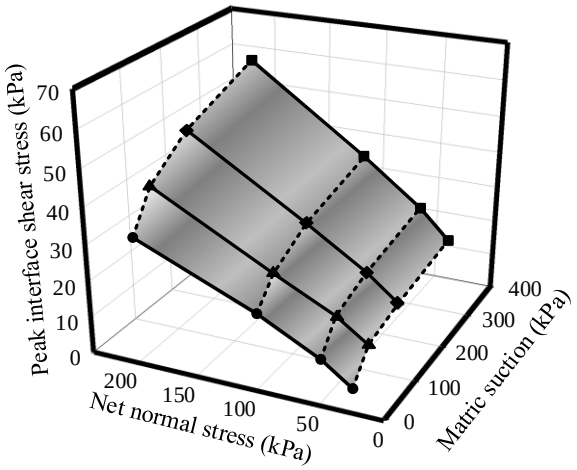

Fig. 7 Development of peak interface shear strength with normal stress and matric suction

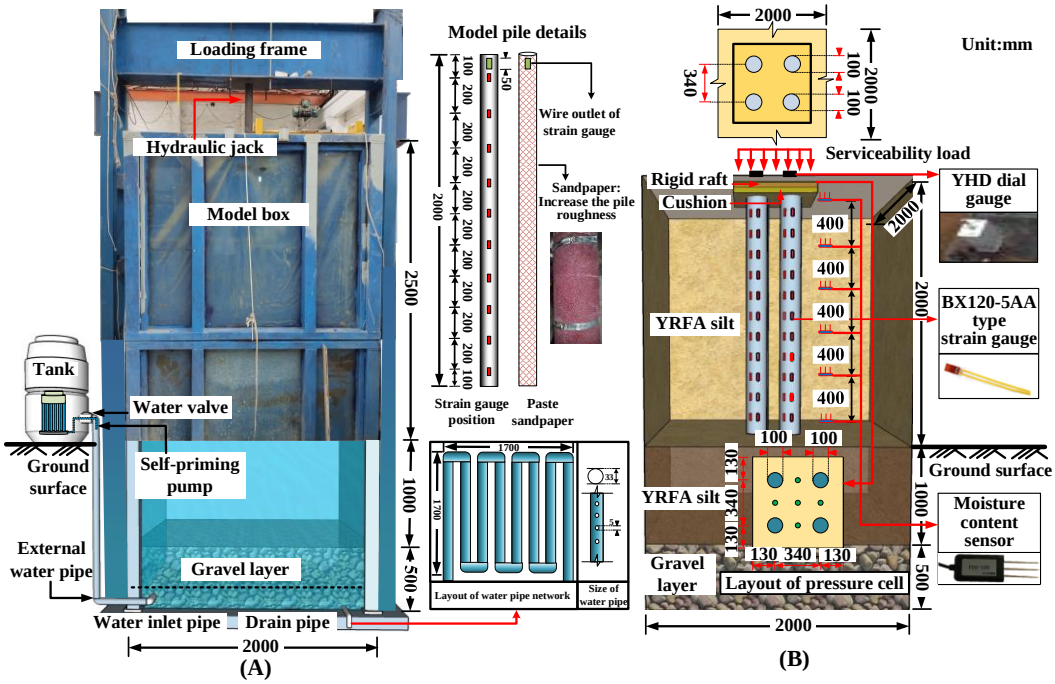

Fig. 8 The newly designed testing box for the RPCF test and corresponding experimental settings

Fig. 8(a). A customized waterproof tarpaulin was placed inside a steel model box. The drainage outlets and drainage networks were set at the bottom of the box. 500 mm thick gravel and double layer geotextile were placed above the drainage pipe network. A self-priming pump was set in the water tank to adjust the GWL.

Inside the model box, it was divided into two layers: the lower layer consisted of 1000 mm-thick YRFA silt placed under pile end, while the upper layer consisted of 2000 mm-thick YRFA silt placed between piles. The soil was compacted in the box by 30 layers with a water content of 14%. Each layer had a thickness of 100 mm corresponding to a wet density of 1824 kg/m^3. The amount of silt used in each layer was calculated in advance a waterproof ruler was pasted on the inner wall of the testing tank to measure the height of the soil during compaction. After each soil layer was compacted, the surface was scarified using a spatula to achieve a corrugated surface and facilitate in achieving a close contact between adjacent compacted soil layers. It is noteworthy that in the process of compaction of soil between piles, a 50 mm high four-hole steel mold was used as compaction plate, whose aperture was a little larger than the diameter of the pile to satisfy the needs of soil compaction and pile fixation. Finally, the model box was sealed by plastic film to prevent evaporation of water. After standing for 7days, the soil can be fully dense under the action of self-weight.

The dimensions of RPCF and experimental settings are illustrated in Fig. 8(b). A four-pile composite foundation was buried inside the YRAP silt. From the top to the bottom, the raft of the composite foundation was assumed to be rigid so that a steel plate was used. The cushion was a 50 mm thick

coarse sand layer.

The prototype for the rigid pile composite foundation was constructed of C25 concrete, with the elastic modulus of 25GPa, a diameter D of 500 mm, an area replacement ratio of 0.086, and a length L of 10000 mm. In previous research, the selection of materials for rigid pile composite foundations has typically relied on two similar basic dimensions: the elastic modulus E and the pile length L (Guo 2021, Chen 2020). Since the pile is primarily subject to vertical force, the compression modulus E is a critical factor in the design of model tests. The similarity ratio for pile length L and elastic modulus E are both 1. The similarity ratio for the compression modulus λ_{EA} must satisfy the following formula

$$\lambda_{EA} = \lambda_E \lambda_A = (\lambda_L)^3 \tag{3}$$

Based on the test conditions, the model pile was made using an aluminum pipe with a diameter of 100 mm, a wall thickness of 5 mm, the elastic modulus of 70 GPa, and a length of 2000 mm. this similarity ratio was calculated using Eq. (4).

$$\lambda_{EA} = \frac{E_p A_p}{E_m A_m} = \frac{70\times10^9}{25\times10^9} \times \frac{\pi\times0.25\times0.25}{\pi\times0.045\times0.045} = 86.4 \approx (\lambda_L)^3 \tag{4}$$

Considering the area replacement ratio of the prototype pile to be 0.086, the influence area of single pile was calculated as following

$$\frac{\pi D^2}{4\times0.0873} = \frac{3.14\times100^2}{4\times0.0873} = 89920 mm^2 \tag{5}$$

Therefore, pile spacing was set as 340mm, which was within the reasonable range of 2~6 times the diameter of the pile, as suggested by Noman (2019). The real time changes of the bearing behaviors of RPCF were monitored through a series of sensors including the strain gauges for pile axial force, dial gauge for total settlement and various earth pressure cells for pile head load, pile base resistance and soil stress under the cushion. In the GWL fluctuation stage, numerous moisture content sensors were buried at different depth to monitor the water content variations. Combined with SWCC shown in Fig. 5, the matric suction profile at different time can be acquired.

Prior to the GWL fluctuation test, static load tests were performed to determine the bearing capacity. For this tests, soil of natural water content (14%) was filled inside the testing tank and compacted to a dry density of 1600 kg/m^3. According to Technical Regulation on Building Ground Treatment (JGJ79—2012), the characteristic value of RPCF bearing capacity indicating the maximum allowable service load was measured as 59 kPa.The characteristic value of RPCF bearing capacity which is also the maximum allowable service load was determined according to the Technical Regulation on Building Ground Treatment (JGJ79—2012).When the ratio of cumulative settlement of composite foundation to the width of bearing plate is 0.1, the corresponding stress is determined as the characteristic value of bearing capacity. Fig. 9 shows the load displacement response of the static load tests, which indicates the characteristic value of RPCF bearing capacity is 59 kPa. In the following test, this value was used as the maximum allowable service load.

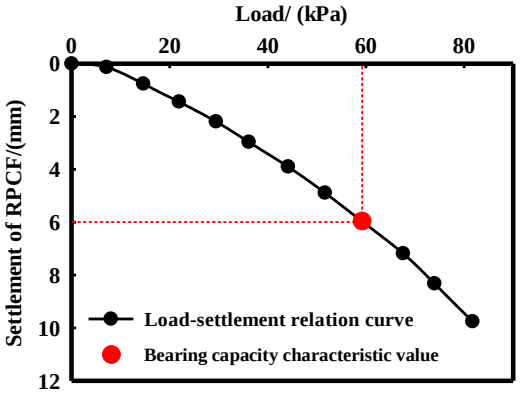

Fig. 9 Load-settlement curve of the RPCF

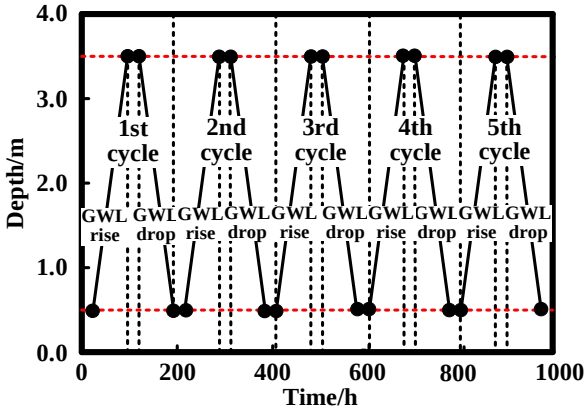

Fig. 10 Variations of GWL with time in the testing process

3.1.3 Experimental process

In the static loading stage, the RPCF finally showed a settlement of 6mm under the vertical stress of 59 kPa, after standing still for 7days. Then the GWL fluctuation process started. The variation of GWL with time was shown in Fig. 10. More specifically, both the GWL rise and drop speed was controlled as 0.042 m/h and the GWL fluctuated between 0.5 m and 3.5 m. After the completion of each single GWL rise and drop, the GWL was kept until the settlement changes was less than 1mm per 12hours. In this process, real time measurement was performed on both bearing behaviors of RPCF (including total settlement, pile head load, pile base resistance, pile axial force and soil stress under the cushion) as well as the soil water content variations.

3.2 Experimental results analysis

3.2.1 Changing disciplines of the RPCF bearing behaviors

Fig. 11 shows the development of the RPCF settlement with time. Apparently continuous and irreversible RPCF settlement occurs during the GWL fluctuation process. The first cycle contributed to near 90% of the total settlement. After five cycles, the settlement gradually stabilized at around 429 mm. Fig. 12 shows that for the first GWL rise which continued for 72 hours, the RPCF settlement quickly increased to around 382 mm.

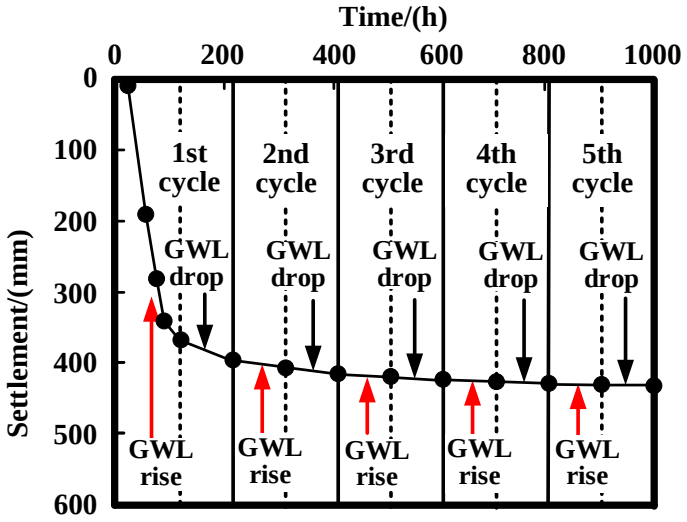

Fig. 11 Variation of the total settlement of composite foundation with GWL fluctuations

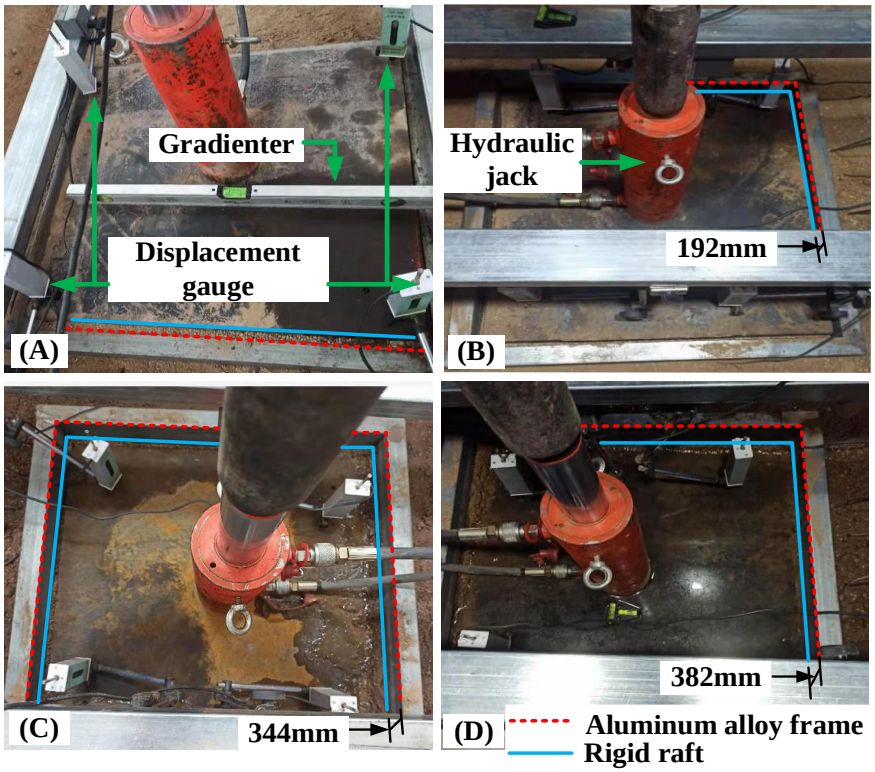

Fig. 12 Settlement of RPCF during the first GWL rise: (a) Initial state, (b) After 48hs, (c) After 72hs and (d) GWL rises to the ground surface

The influence of GWL fluctuations on upper load sharing ratio between piles and soil is demonstrated in Fig. 13. Initially, the soil between piles borne relatively large loads of the upper load, which accounted for around 35.3%. The load borne by piles accounted for around 64.7%. After the first GWL rise, the proportion of upper load borne by the piles soon increased to around 91.3%, while the proportion taken by soil dropped to 8.7%. In the following GWL changes, both the pile load sharing ratio increasing and soil load sharing ratio decreasing trend continued, but only minor changes were observed.

Figs. 14 and 15 show the changes of pile axial force and shaft friction in the GWL fluctuation process. The static loading stage lasted for 24hs, after which each single GWL rise and drop process lasted for around 72hs, respectively. In the static loading stage, the pile head load was relatively small and the neutral surface was in the lower part of the pile. While in the first GWL rise, the pile head load experienced a increment by 27%. Also, both the positive friction in the lower part of pile and the negative friction along the upper part of the pile decreased significantly. The neutral surface moved up to a

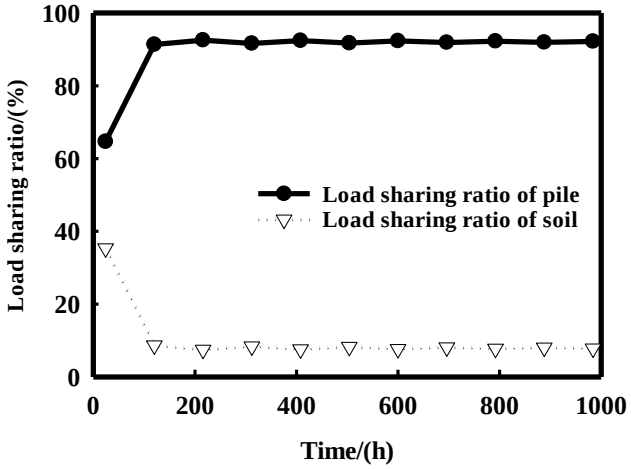

Fig. 13 Pile and soil load sharing ratio variations in GWL fluctuations

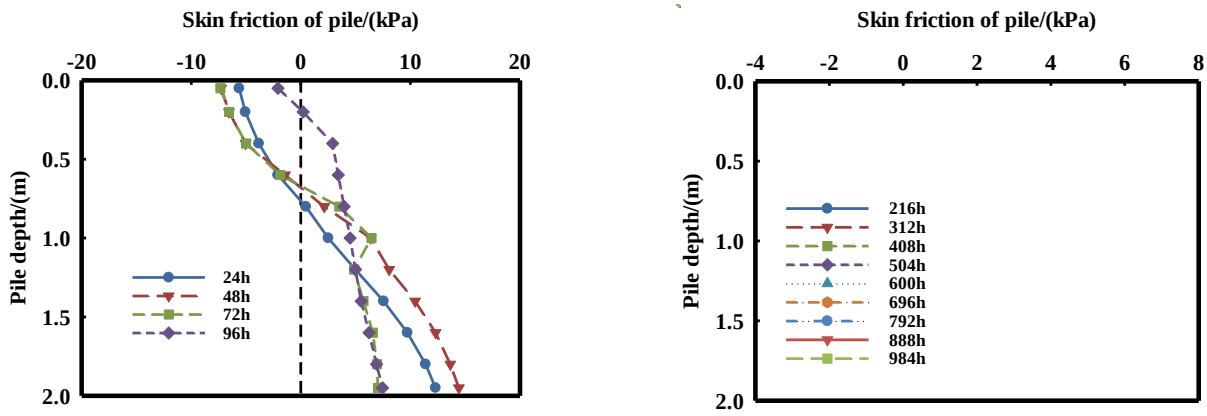

(a) The first GWL rise (b) The first GWL drop and other cycles

Fig. 14 Pile shaft friction variations in GWL fluctuation cycles

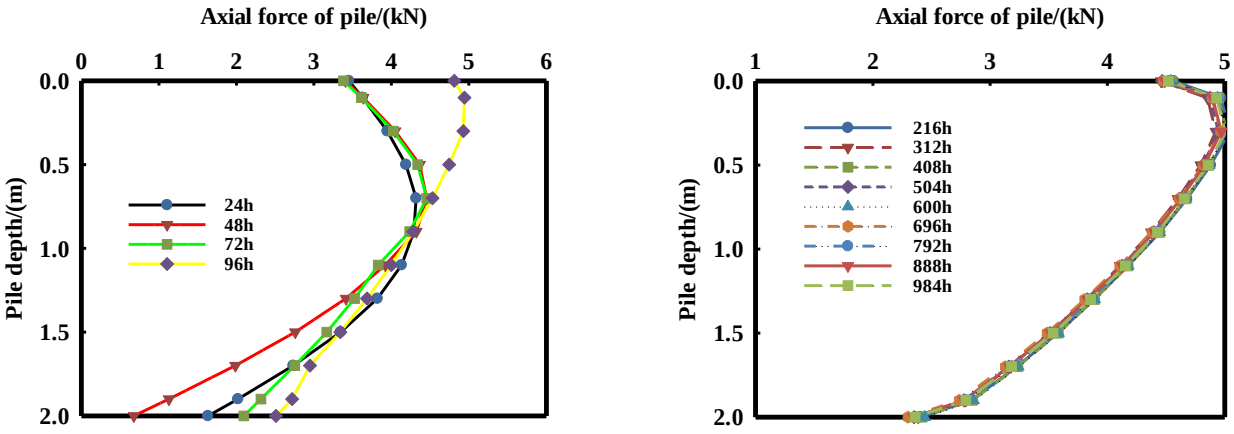

(a) The first GWL rise (b) The first GWL drop and other cycles

Fig. 15 Pile axial force variations in GWL fluctuation cycles

position close to the pile head. In the following GWL fluctuations, the pile head load, pile shaft friction and pile base resistance also increased but the magnitude was minor. After five GWL rise and drop cycles, finally the pile head load gained an increment by around 29%.

3.2.2 Changing mechanisms of RPCF bearing behaviors

The reasons responsible for the RPCF bearing behaviors changes can be attributed to the matric suction and degree of

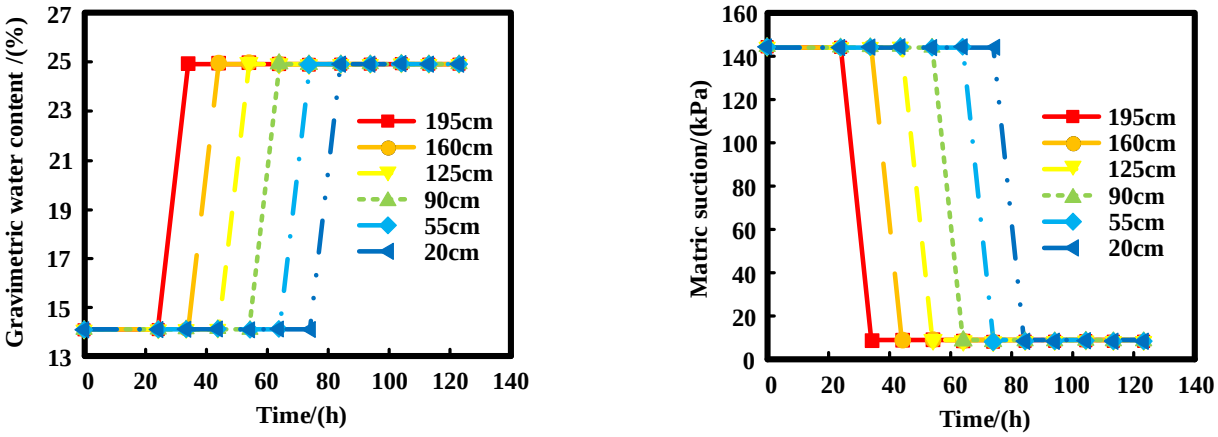

(a) (b)

Fig. 16 Variations of soil gravimetric water content (a) and matric suction (b) in the first GWL rise process

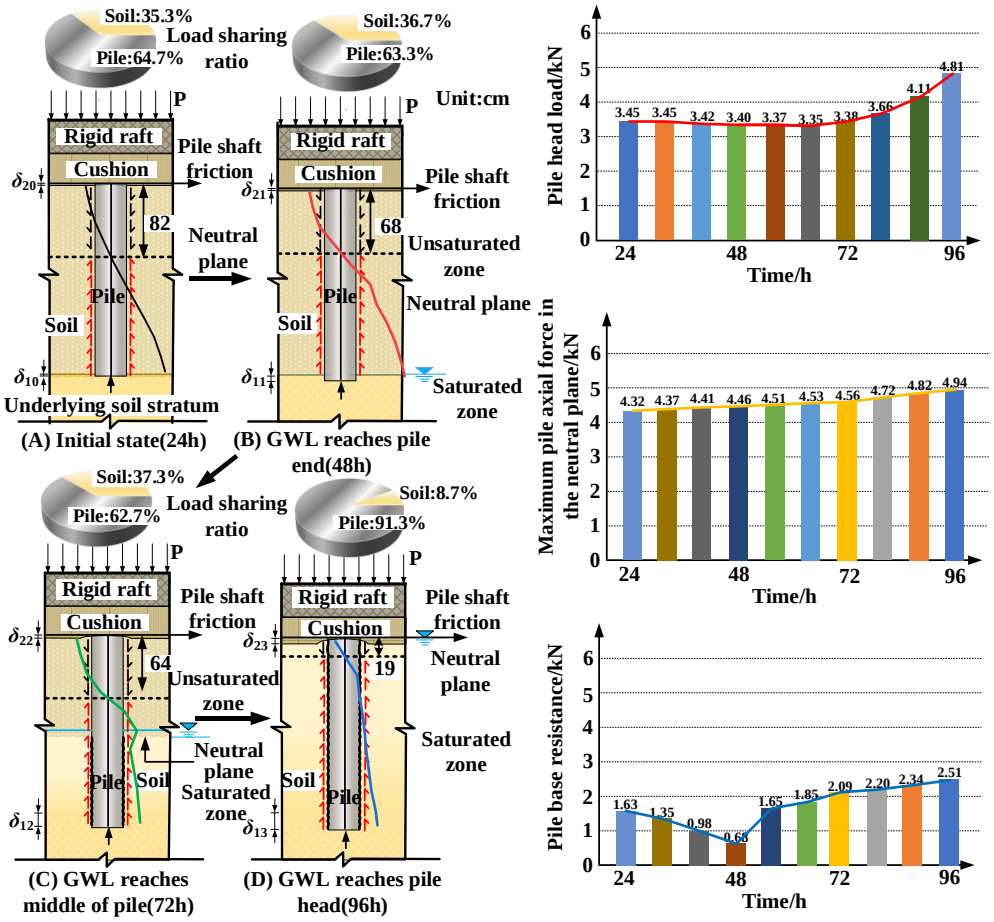

Fig. 17 RPCF mechanical behaviors changing mechanism during the first GWL rise

saturation changes of soil in the GWL fluctuation process. More specifically, the major RPCF settlement appeared in the first GWL rise and drop process. Fig. 16 shows the gravimetric water content and matric suction changes in the first GWL rise process with time, which indicates the matric suction suffered a sudden decrease in the GWL rising proces

Fig. 17 shows the mechanical behaviors variations of the RPCF in the GWL fluctuation process. As shown in Fig. 17(a) and 17(b), as the GWL rose to the bottom of the RPCF, both the stiffness and shear strength of the underlying soil stratum sharply decreased due to matric suction reduction (Vanapalli 1996, Oh and Vanapalli 2010). As a result, the compression deformation of the underlying soil stratum increased significantly and contributed to the RPCF settlement. Piles produced greater downward displacement relative to soil between piles. The position of the neutral surface moved

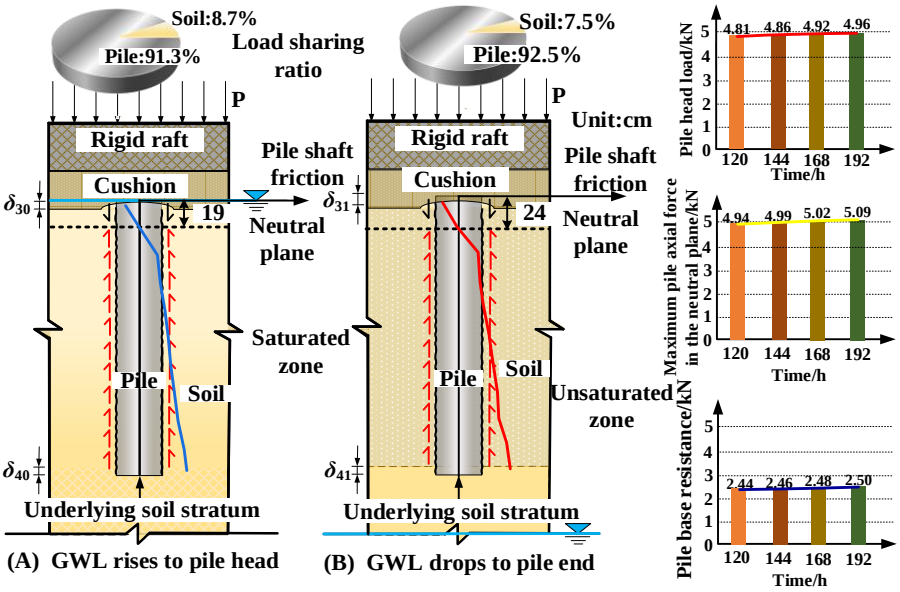

Fig. 18 RPCF mechanical behaviors changing mechanism during the first GWL drop

upward from 82 cm to 68 cm. In this process, the load sharing ratio of the piles slightly decreased from 64.7% to 63.3% (i.e., from 13.86 kN to 13.56 kN). However, the pile base resistance decreased from 1.63 kN to 0.68 kN, which was contributed to the increase of the distribution zone in the positive friction zone.

While before the GWL rose to the middle of reinforcement zone, as shown in Fig. 17(c), the load sharing ratio of the piles was in a brief fluctuating state from 63.3% to 62.7% (i.e., from 13.56 kN to 13.43 kN). In this state, the soil stiffness between piles in already saturated zone sharply decreased and resulted in significant compression deformation. And the positive friction below the neutral surface decreased dramatically due to the vanishment of the contribution of matric suction to the pile shaft friction and resulted in significant pile penetration depth into underlying soil stratum. In other words, both the ability of the soil between piles in the already saturated zone and piles were weakened. That is also the reason for the position of the neutral surface varied from 68 cm to 64 cm. Also, since the dramatical decrease of positive friction zone below the neutral surface, the pile base resistance increased from 0.68 kN to 2.09 kN.

Upon fully saturation, as shown in Fig. 17(d), both negative friction above the neutral surface and the positive friction below it decreased significantly. The soil between piles in the reinforcement zone was subjected to more significant compression deformation. Consequently, the position of neutral surface further moved upward from 64cm to 19cm, which significantly enlarged the positive friction distribution zone. The pile-soil relative displacement increments also contributed to the fully mobilization of the pile shaft friction. In this process, the pile load sharing ratio increased dramatically from 62.7% to 91.3% (i.e., from 13.43 kN to 19.66 kN), which leaded to significantly increment in pile soil stress ratio. In this process, the pile base resistance increased from 2.09 kN to 2.51 KN.

As the GWL dropped, the effective stress of the soil between piles gradually increased, resulting in consolidation settlement. In this process, the seepage force also contributed to the RPCF settlement to some extent. Consequently, the ability of the soil between piles to bear the upper load further weakened and the pile load sharing ratio further increased, as shown in Fig. 18. Both the pile penetration depth into the cushion and underlying stratum increased, which indicating higher pile head load and pile base resistance. Both the negative friction in the upper part and the positive friction in the lower part of pile increased. The neutral surface further moved downward slightly. On the micro level, the RPCF settlement developed in the GWL drop process could be attributed to the flow away of fine particles inside the YRAP silt and the rearrangement of the silt particles. Obviously, such settlement was plastic settlement and irreversible.

In the following GWL fluctuation cycles, the mechanical properties of the soil changed periodically with the variations of pore water pressures. The RPCF settlement kept increasing, but the increment became increasingly minor from 13 mm in the second cycle to nearly 1mm in the fifth cycle. In this process, the load sharing ratio of the pile increased gradually and slightly from 91.3% to 92.5%. In other words, after the first GWL rise and drop, further GWL fluctuations posed minor influences on the bearing behaviors of the RPCF. From the micro perspective, such phenomenon could be attributed to the fact that the flow away of the fine particles and the rearrangement of the large particles continued until a stable soil structure was eventually formed.

4. Revised composite modulus method for the RPCF settlement estimation

As discussed above, more than 90% of the RPCF settlement generated in the first GWL rise process. In the following GWL fluctuation process, the RPCF settlement only

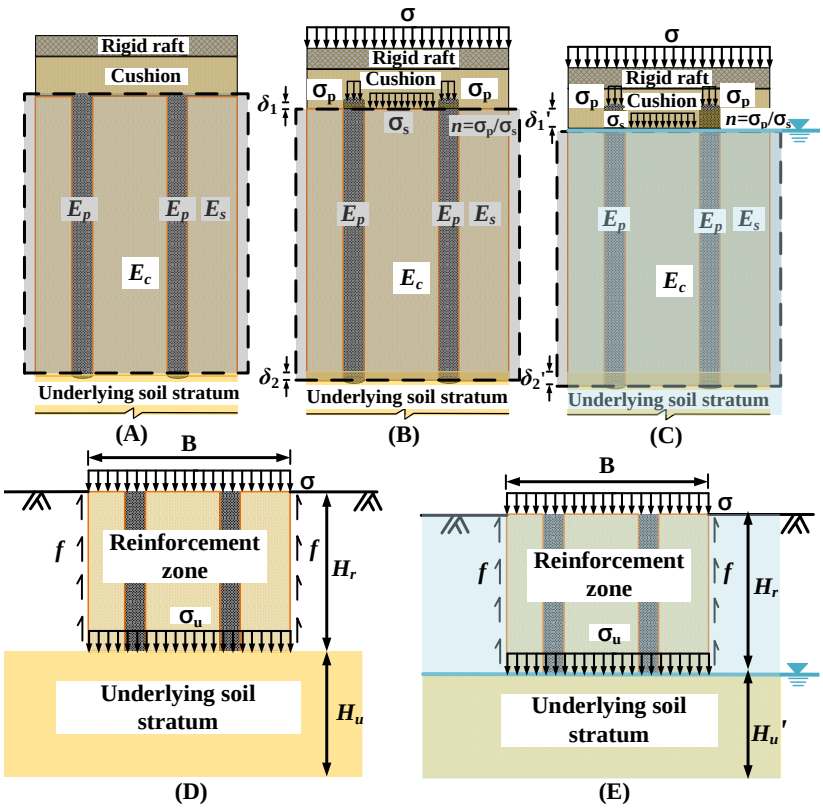

Fig. 19 Schematic of the composite modulus method for RPCF settlement calculation

increased slightly. In other words, major attentions should be concentrated on the RPCF settlement caused by the first GWL rise.

According to Chinese Technical Standard on Building Ground Treatment (JGJ79-2012), the total RPCF settlement could be calculated as the sum of the compression deformation of the composite foundation in the reinforcement zone and the underlying soil stratum, as shown in Eq. (6).

$$S_T = S_R + S_U \tag{6}$$

Where S_R and S_U are the compression deformation of the composite foundation in the reinforcement zone and the compression deformation of the underlying soil stratum.

As shown in Figs. 19(a) to 19(C), considering the piles and soil between piles in the reinforcement zone as a whole, corresponding compression deformation (S_R) could be calculated through Eq. (7) using the composite modulus, as indicated in Eq. (8).

$$S_R = \frac{\sigma H_r}{E_c} = \frac{\sigma H_r}{[1+m(n-1)]E_s} \tag{7}$$

$$E_c = [1+m(n-1)]\alpha E_s' = [1+m(n-1)]E_{unsat} \tag{8}$$

where m is the area replacement rate; E_s' is the compression modulus of soil between piles, E_s is the compression modulus of the YRAP silt and n is the pile-soil stress ratio; σ is the average additional stress of composite foundation; E_c is the composite elastic modulus; H_r is the thickness of reinforcement zone.

As for the compression deformation of the underlying soil stratum, initially the additional stress could be estimated using the equivalent box foundation method. In other words, the piles and soil between piles in the reinforcement zone was equivalent to a box foundation, as shown in Figs. 19(d) and 19(e). Then the additional stress acting on the top of the underlying soil stratum could be calculated using Eq. (9) through force equilibrium condition and the compression deformation of underlying soil stratum could be calculated using Eq. (10) by layer-wise summation method.

$$\sigma_u = \sigma - \frac{2(B+D)H_r f}{BD} \tag{9}$$

$$S_U = \frac{\sigma_u H_u}{E} \tag{10}$$

where σ_u is the additional stress at the top of substratum; B is the width of the composite foundation; D is the pile spacing; f is the density of the equivalent side friction ($f=\zeta K\tan\delta'\sigma'_{v0}$, Wu *et al.* 2016, Lang *et al.* 2022); Hu is the thickness underlying soil stratum.

When the GWL rises, both the stiffness of the soil in the underlying soil stratum and reinforcement zone deteriorates. Combined with the semi-empirical model (Eq. (11)) proposed by Oh *et al.* (2009) for estimation of unsaturated soil elastic modulus, Eqs. (7) and (10) could be revised to Eqs. (12) and (13), respectively. Considering the GWL may locate in the middle of the reinforcement zone or underlying soil stratum, the layer-wise summation method should be used.

Table 3 Various parameters used for the calculation of the composite foundation settlement S_T

E_{unsat}/MPa	$(u_a$-$u_w)$ /kPa	S_r/%	n	E_{sat}/MPa	E_c/MPa	σ/kPa	S_R/mm
					0.62	59	189.27
2.48	162.43	0.57	49.53	0.145	f/kPa	σ_u/kPa	S_U/mm
					4.32	29.3	202.09

$$E_{unsat} = E_{sat}\left[1+\alpha\frac{(u_a-u_w)}{(P_a/100)}(S^{\beta})\right] \quad (11)$$

where E_{unsat} is the modulus of elasticity under unsaturated condition; E_{sat} is the modulus of elasticity under saturated condition; S is the degree of saturation; $(u_a$-$u_w)$ is the matric suction under unsaturated condition; α, β are the fitting parameters; P_a is the atmospheric pressure (i.e., 100 kPa).

$$S_R = \frac{\sigma H_r}{E_c} = \frac{\sigma H_r}{[1+m(n-1)]E_{unsat}}\left[1+\alpha\frac{(u_a-u_w)}{(P_a/100)}(S^{\beta})\right] \quad (12)$$

$$S_U = \frac{\sigma_u H_u}{E_{unsat}}\left[1+\alpha\frac{(u_a-u_w)}{(P_a/100)}(S^{\beta})\right] \quad (13)$$

Table 3 shows the various parameters used for the calculation of the RPCF settlement. For fine grained soil, such as the expansive soils, when plasticity index I_p is higher than 16%, the fitting parameter α should range from 0.05 to 0.15 and the fitting parameter β is 2 (Adem and Vanapalli 2015). However, for the unsaturated YRAP silt, according to the oedometer test results, the fitting parameter α and β are determined as 0.3 and 2, respectively.

Introducing all these parameters into calculation, the composite foundation settlement was estimated to be 391.37 mm, which was a little higher than the experimental data of 382 mm. A more conservative estimation well indicates the feasibility of the revised composite modulus method. Further, the proposed method only requires inputting parameters including the soil index properties, saturated elastic modulus, SWCC and matric suction profiles, which can be easily obtained from lab test and site investigations. After estimating the RPCF settlement caused by matric suction reduction in the first GWL rise process, the total RPCF settlement after cyclic GWL fluctuations and in the stable state can be estimated according to the proportions. For current study, an amplify factor of 10% was suggested.

5. Conclusions

Due to high particle roundness and poor particle gradation, the mechanical properties of silt in YRAP will significantly deteriorate with increasing water content. Under GWL fluctuations induced by extreme weather conditions like heavy rains and drought, the RPCF constructed in YRAP will suffer the degradation of bearing behaviors and additional settlement.

In order to reveal the changing disciplines and inherent mechanisms of the RPCF bearing behaviors under GWL fluctuations, a large-scale model test was designed and performed. By analyzing the experimental results, following conclusions can be summarized.

The settlement of the RPCF gained a sharp increment of 382 mm in the first GWL fluctuation cycle and then gradually stabilized to 429 mm in the following cycles. In the first GWL rise process, the load sharing ratio of pile increased dramatically from 64.7% to 82.6%. Both the negative friction above the neutral surface and the positive friction below the neutral surface decreased enormously. The neutral surface rose from 0.82 m to 0.19 m. In the GWL drop process, the pile load sharing ratio continued increasing but the growth amplitude was only 2%. The RPCF settlement developed in GWL rise process could be attributed to the gradual deterioration of the mechanical properties of soil in the underlying soil stratum and reinforcement zone. When the matric suction decreased, the shear strength of soil and pile-soil interface degraded as well as the soil stiffness. The RPCF settlement developed in GWL drop process could be attributed to the flow away of fine particles inside the YRAP silt and the rearrangement of the silt particles. In the following GWL fluctuation process, soil particle rearrangement continues until a stable inner structure of soil was eventually formed.

The composite modulus method for RPCF settlement predictions was modified to be applied in unsaturated YRAP. Combined with the semi-empirical model proposed by Oh *et al.* (2009) for estimation of unsaturated soil elastic modulus, the deterioration of the soil stiffness in the reinforcement zone and underlying soil stratum was considered. Reasonably good comparisons were achieved between the estimation using the proposed method and the experimental data. The proposed method is relatively simple which only needs limited number of input parameters including the average additional stress, matric suction profile and compression modulus of soil in the substratum and reinforcement zone. In engineering practice, reasonable estimations of the RPCF settlement subjected to GWL fluctuations could be achieved quickly and conveniently through the proposed method without complex load transfer analysis

Acknowledgements

The first author, Yunlong Liu, thanks the department of Science and Technology of China for funding the project entitled “Research on lateral earth pressure of expansive soil upon wetting considering the cumulative damage effect of dry-wet cycles”-Fund code: 42107196 for the period 2022-01 to 2024-12.

References

Adem, H.H. and Vanapalli, S.K. (2015), "Prediction of the modulus of elasticity of compacted unsaturated expansive soils", *Int. J. Geotech. Eng.*, **9**(2), 163-175. https://doi.org/10.1179/1939787914y.0000000050.

Ajdari, M. and Esmail, A.P. (2015), "Experimental evaluation of the influence of the level of the ground water table on the bearing capacity of circular footings", *Iranian J. Sci. Tech. Transact. Civil Eng.*, **39**(2), 497-510. https://doi.org/10.22099/IJSTC.2015.3516.

Alencar, A., Galindo, R. and Melentijevic, S. (2021), "Influence of the groundwater level on the bearing capacity of shallow foundations on the rock mass", *Bull. Eng. Geol. Environ.*, **80**(9), 6769-6779.

An, L.Z., Quan, S. and Xu, Y. (2013), "Dynamic characteristics of the shallow groundwater table and its genesis in the Yellow River Delta", *Environ. Sci. Technol.*, **36**(9), 51-56.

ASTM (American Society for Testing and Materials). (2010), "Standard test methods for liquid limit, plastic limit, and plasticity index of soils", ASTM D4318-10ε1, ASTM international, West Conshohocken, Pa.

ASTM (American Society for Testing and Materials). (2012), "Standard test methods for laboratory compaction characteristics of soil using standard effort (12 400 ft-lbf/ft3(600 kN-m/m3))", D698-12ε2 , ASTM international, West Conshohocken, Pa.

ASTM (American Society for Testing and Materials). (2014), "Standard test methods for specific gravity of soil solids by water pycnometer", ASTM D854-14, ASTM international, West Conshohocken, Pa.

ASTM (American Society for Testing and Materials). (2016), "Standard test methods for determination of the soil water characteristic curve for desorption using hanging column, pressure extractor, chilled mirror hygrometer, or centrifuge", ASTM D6836-16, ASTM international, West Conshohocken, Pa.

Ausilio, E. and Conte, E. (2005), "Influence of groundwater on the bearing capacity of shallow foundations", *Can. Geotech. J.*, **42**(2), 663-672. https://doi.org/10.1139/t04-084.

Bie, Y.S., Liu, M.Y. and Zhang, Q. (2014), "Numerical and stress analysis of composite foundation with long and short piles for the Hong Kong-Zhuhai-Macao bridge", *J. Wuhan Univ. Tech.*, **36**(5), 101-105.

Cai, J., Du, G., Xia, H. and Sun , C. (2021), "Model test and numerical simulation study on bearing characteristics of pervious concrete pile composite foundation", *KSCE J. Civil Eng.*, **25**(10), 3679-3690. https://doi.org/10.1007/s12205-021-1522-7.

Chen, J., Chen, W., Zhang, K. and Li, L. (2019), "The application of CFG pile composite foundation in the reconstruction of the Dujiangyan", IOP Conference Series: Earth and Environmental Science, vol. 300, Article ID 022159. https://doi.org/10.1088/1755-1315/300/2/022159.

Cheng, Z. and Deng, Y. (2020), "Bearing characteristics of moso bamboo micropile-composite soil nailing system in soft soil areas", *Adv. Mater. Sci. Eng.*, **2020**, 1-17. https://doi.org/10.1155/2020/3204285.

Cheng, R.M. (2001), "Review article: Silt and the future development of China's Yellow River", *Geograph. J.*, **167**(1), 7-22. https://doi.org/10.1111/1475-4959.00002.

Dong, R. (2016), "Analysis of influence of groundwater level change on vertical bearing capacity characteristic value of CFG single pile", M.S. thesis, Zhengzhou University, Zhengzhou, China.

Fredlund, D.G. and Xing, A. (1994), "Equations for the soil-water characteristic curve", *Can. Geotech. J.*, **31**(4), 521-532. https://doi.org/10.1139/t94-061.

Fan, W.Y. (2007), "Research on experiments for silt engineering characteristic sat inundated area", *Railway Investigation Survey*, **33**(6), 14-17.

Fu, L. (2019), "Study on influence of groundwater level change on pile foundation of high-speed railway viaduct", M.S. thesis, Zhejiang University, Hangzhou, China.

Fu, Q. and Li, L. (2020), "Vertical load transfer behavior of composite foundation and its responses to adjacent excavation: centrifuge model test", *Geotech. Test. J.*, **44**(1). https://doi.org/191-204. 10.1520/gtj20180237.

Guo, Y., Lv, C., Hou, S. and Liu, Y. (2021), "Experimental study on the pile-soil synergistic mechanism of composite foundation with rigid long and short piles", *Math. Probl. Eng.*, 1-15. https://doi.org/10.1155/2021/6657116.

Hamid, T. B. and Miller, G.A. (2009), "Shear strength of unsaturated soil interfaces", *Can. Geotech. J.*, 46(5), 595-606. https://doi.org/10.1139/t09-002.

Hansen, B., Denver, H. and Petersen, K. (1987), "The influence of groundwater on bearing capacity of footings", *Proceedings of the 9th European Conference on Soil Mechanics and Foundation Engineering*, Dublin, Ireland, August/September 1987.

Jin, Q., Zheng, Y., Cui, X., Cui, S., Qi, H., Zhang, X. and Wnag, S. (2020), "Evaluation of dynamic characteristics of silt in Yellow River Flood Field after freeze-thaw cycles", *J. Central South Univ.*, **27**(7), 2113-2122. https://doi.org/10.1007/s11771-020-4434-7.

Kumar, J. and Chakraborty, D. (2013), "Bearing capacity of foundations with inclined groundwater seepage", *Int. J. Geomech.*, **13**(5), 611-624. https://doi.org/1943-5622.0000241.

Lang, R., Xiong, H., Sun, L. and Yadong, Z. (2021), "A simplified prediction method for additional stress on underlying layer of rigid pile-net composite foundation", *Eur. J. Environ. Civil Eng.*, 1-20. https://doi.org/10.1080/19648189.2021.1916603.

Li, M., Li, Y.H.., Lv, M.F. and Guo, Y.C. (2022), "Comparative shear test study on silt-concrete interface and silt", *Chinese J. Undergr. Sp. Eng.*, **18**(1), 171-178.

Liu, B.S., Zhang, Y.J. and Wang, X. (2016), "Analysis on influencing factors of collapsibility of artificially prepared sand", *J. Railway Sci. Eng.*, **13**(10), 1933-1939.

Liu, P., Yang, G.H., Fan, Z. and Sun, Y.C. (2016), "Cushion effects on the bearing gapacity behaviors of the rigid pile composite foundation", *J. Civil Eng. Management*, **32**(2), 13-18.

Liu, P., Yang, G.H. and Fan, Z. (2016), "Experimental study on size effect of rigid pile composite foundation", J. Rock Mech. Geotech. Eng., **35**(1), 187-200.

Lu, D., Li, X., Du, X., Lin, Q. and Gong, Q. (2020). "Numerical simulation and analysis on the mechanical responses of the urban existing subway tunnel during the rising groundwater", *Tunn. Undergr. Sp. Tech.*, **98**, 103297. https://doi.org/10.1016/j.tust.2020.103297.

Luo, F.R., Liu, C.W. and Han, X. (2011), "Influence of groundwater level rise on subway tunnel structure", *China Railway Sci.*, **32**(1), 81-85.

Li, Y., Lei, X.W., Meng, Q.S., Chen, J. and Zhang, L. (2018), "Experimental study on shear strength of remolded basalt residual soil", J. Hefei Univ. Tech. (Natural Science), **41**(2), 240-244+265.

Ma, T.Z., Zhu, Y., Yang, X. and Ling, Y. (2018), "Bearing characteristics of composite pile group foundations with long and short piles under lateral loading in loess areas", *Math. Probl. Eng.*, 2018.

National standard of the people's republic of China (JGJ 79—2012). (2012), Technical code for ground treatment of buildings. China Architecture & Building Press.

Noman, B.J., Abd-Awn, S.H. and Abbas, H.O. (2019), "Effect of pile spacing on group efficiency in gypseous soil", *Civil Eng. J.*, **5**(2), 373-389.

Oh, W.T., Vanapalli, S.K. and Puppala, A.J. (2009), "Semi-empirical model for the prediction of modulus of elasticity for unsaturated soils", *Can. Geotech. J.*, **46**(8), 903-914. https://doi.org/10.1139/t09-030.

Oh, W.T. and Vanapalli, S.K. (2010), "Influence of rain infiltration on the stability of compacted soil slopes", *Comput. Geotech.*, **37**(5), 649-657. https://doi.org/10.1016/j.compgeo.2010.04.003.

Pan, M. (2018), "Experimental study on shear strength characteristics of typical loess in Taiyuan", M.S. thesis, Taiyuan University of Technology, Taiyuan, China.

Park, D., Kim, I. and Kim, G. (2017), "Groundwater effect factors for the load-carrying behavior of footings from hydraulic chamber load tests", *Geotech. Test. J.*, **40**(3), 440-451.

Park, D., Kim, I., Kim, and G. and Lee, J. (2019), "Effect of groundwater fluctuation on load' carrying performance of shallow foundation", *Geomech. Eng.*, **18**(6), 575-584. https://doi.org/10.1520/gtj20160078.

Reddy, A.S. and Manjunatha, K. (1997), "Influence of water table on bearing capacity of adjacent strip footings on sand exhibiting anisotropy", *Soil Found.*, **37**(1), 53-64. https://doi.org/10.3208/sandf.37.53.

Safarzadeh, Z. and Aminfar, M.H. (2019), "Experimental and numerical modeling of the effect of groundwater table lowering on bearing capacity of shallow square footings", *Int. J. Eng.*, **32**(10), 1429-1436. https://doi.org/10.5829/ije.2019.32.10a.12.

Schnellmann, R., Rahardjo, H. and Schneider, H.R. (2013), "Unsaturated shear strength of a silty sand", *Eng. Geol.*, **162**, 88-96. https://doi.org/10.1016/j.enggeo.2013.05.011.

Sharma, B., Sarkar, S. and Hussain, Z. (2019), "A study of parameters influencing efficiency of micropile groups", Ground Improvement Techniques and Geosynthetics. Springer, Singapore, 11-18. https://doi.org/10.1007/978-981-13-0559-7_2.

Song, X.G., Zhang, H.B., Wang, S.G., Jia, Z.X. and Guan, Y.H. (2010), "Hydrophilic characteristics and strength decay of silt roadbed in Yellow River alluvial plain", *Chinese J. Geotech. Eng.*, **32**(10), 1595-1602.

Sun, X.H. (2010), "Effect of foundation rigidity and cushion thickness on rigid pile Composite Foundation bearing capacity", MS thesis, China Academy of Building Research, Beijing, China.

Vanapalli, S.K., Fredlund, D.G., Pufahl, D.E. and Clifton, A.W. (1996), "Model for the prediction of shear strength with respect to soil suction", *Can. Geotech. J.*, **33**(3), 379-392. https://doi.org/10.1139/t96-060.

Vanapalli, S.K. and Mohamed, F.M.O. (2007), "Bearing capacity of model footings in unsaturated soils",. In proceedings, International Conference "From Experimental Evidence towards Numerical Modeling of Unsaturated Soil", Weimar, Germany, unsaturated Soils: Experimental Studies: 483-493. https://doi.org/10.1007/3-540-69873-6_48.

Veiskarami, M. and Kumar, J. (2012), "Bearing capacity of foundations subjected to groundwater flow", *Geomech. Geoeng.*, **7**(4), 293-301. https://doi.org/10.1080/17486025.2011.631038.

Sharma, V.J., Vasanvala, S.A. and Solanki, C.H. (2015), "Study of cushioned composite piled raft foundation behaviour under seismic forces", *Aust. J. Civil Eng.*, **13**(1), 32-39. https://doi.org/10.1080/14488353.2015.1092636.

Wang, W.L., Wang, X.M. and Ma, X. (2015), "Experimental study on influence of groundwater on loess pile group foundation", *China J. Highway Transport*, **28**(9), 16-23.

Wu, S.W., Zhu, Z.D. and Zhang, A.J. (2016), "Research on the equivalent solid side friction resistance of rigid pile composite-foundation", *Henan Sci.*, **34**(2), 238-242.

Xiao, J.H., Liu, J.K. and Peng, L.Y. (2008), "Influence of density and moisture content of alluvial silt on mechanical properties of Yellow River", *Rock Soil Mech.*, **146**(2), 409-414.

Xu, A.Q., Yue, J.W. and Song, D. (2017), "Research on compression modulus and effective stress parameter of unsaturated silt in the Yellow River flood area", *Chinese J. Appl Mech.*, **34**(4), 672-678.

Xu, S.J. (2020), "Experimental study on pile-soil load sharing of rigid pile composite foundation under different side load conditions", M.S. thesis, China Academy of Building Research and Tsinghua University, Beijing, China.

Yang, D.J. and Wang T.C. (2010), "Research on settlement mechanism and influence factors of rigid pile composite foundation", *Eng. Mech.*, **27**(1), 150-163.

Yao, Z.Y. (2006), "Engineering properties on Yellow River alluvial-plain soil", MS thesis. Tianjin University, Tianjin, Beijing.

Yu, J. (2022), "Modeling between water resources security and regional economic growth in the Yellow River basin based on entropy weight method-a case study for future smart city", *J. Test. Evaluation*, https://doi.org/10.1520/jte20220053.

Zhang, D., Zhang, Y., Kim, C.W., Meng, Y., Garg, A. and Fang, K. (2018), "Effectiveness of CFG pile-slab structure on soft soil for supporting high-speed railway embankment", *Soils Found.*, **58**(6), 1458-1475. https://doi.org/10.1016/j.sandf.2018.08.007.

Zhang, Y., Zhou, L.P., Wang, M.Y., Ding, X. and Wang, C. (2021), "Experimental study on the negative skin friction of the pile group induced by rising and lowering the groundwater level", *Adv. Civil Eng.*, 2021. https://doi.org/10.1155/2021/2574727.

Zhang, Y.P., Tang, Y.Q. and Xu, J. (2017), "Deformation and settlement mechanism of silt under cyclic water level fluctuation", *J. Tongji Univ*. (natural science), **45**(12), 1773-1782.

Zhao, X. (2014), "The influence of water level change on the dynamic characteristics and cumulative deformation characteristics of high-speed railway subgrade", M.S. thesis, Zhejiang university, Nanjing, China.

IC